Metastable States in Multicomponent Liquid−Solid Systems I: A Kinetic Crystallization Model

Jan H. Los,* Willem J. P. van Enckevort, and Elias Vlieg

Katholieke Universiteit Nijmegen, Toernooiveld, 6525 ED Nijmegen

Eckhard Flöter

Unilever Research Vlaardingen, Olivier van Noortlaan 120, 3133 AT Vlaardingen

Received: March 6, 2002; In Final Form: May 18, 2002

The formation of metastable, inhomogeneous solid solutions during the crystallization of mixed systems is a well-known and often inconvenient phenomenon, which limits the reliability of calculations based on equilibrium. In this paper we present a relatively simple kinetic model that describes the evolution of a crystallization process in a finite, multicomponent system, represented by crystallization curves. The kinetic model is applied to fat mixtures, used as model systems, with up to 10 components, and the resulting metastable states are compared with the equilibrium predictions. The deviations from equilibrium strongly depend on the thermodynamic properties of the individual, pure components, the mixing properties, the presence of a solvent, and the undercooling. Generally it holds that the solid phase fraction predicted by the kinetic model is lower than that of the equilibrium state.

1. Introduction

Mixed crystals[1] represent an important class of materials for application owing to the possibility of tuning their properties by varying the composition. Examples include metal and semiconductor alloys and molecular, mixed crystals. These latter play an important role in separation techniques based on solidification, with applications in the food and pharmaceutical industry.[2]

Usually, to determine the state of a mixed system at a given pressure and temperature (P, T), one assumes that the system is in equilibrium and the equilibrium state is calculated, i.e., the state with the lowest Gibbs free energy. The result of such a calculation is a state with one or more homogeneous phases. For vapor and liquid phases this approach may be adequate because the relatively high diffusion rate in these phases ensures homogeniety within relatively short times. However, in the case of mixed solid phases, the equilibrium state is often not reached due to the very low diffusion rates in solid phases, especially for molecular systems. The composition gradients in the solid phase, which are built in during the crystallization process, persist for long times after an equilibrium has been reached between the remaining liquid and the last grown solid phase at the surface. Hence, on a finite, relevant time scale the final state is not the equilibrium state with homogeneous phases but a metastable state with an inhomogeneous solid phase.

This paper deals with the determination of these metastable states in finite, multicomponent systems. In our modeling, diffusion in the solid phase will be completely neglected. For many molecular systems this is a good approximation, and it holds also for fat systems, which we have used as model systems throughout this work. Even if local rearrangements of molecules may occur within the solid phase, as for example has been shown experimentally for binary, equimolar mixtures of n-parafins where the formation of microphases was observed after deep quenching,[3,4] macroscopic transport may be considered as negligible.

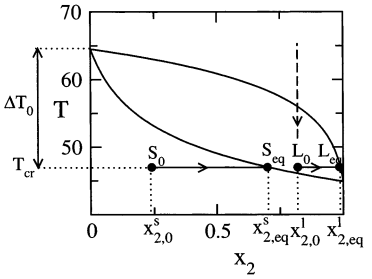

Figure 1. An example of the trajectories that the liquid composition and the corresponding growth composition of the solid-phase traverse with respect to the equilibrium phase diagram of the binary fat mixture with the components PPP (1) and SOS (2). The initial and final liquid compositions are indicated by L_0 and L_{eq}, respectively. The compositions of the first and the last grown solid phase are indicated by S_0 and S_{eq}, respectively.

As an illustration, Figure 1 shows schematically the formation of a metastable state by the trajectories of the compositions of the liquid and the corresponding growing solid phase during isothermal crystallization in a finite, binary system with components 1 and 2. A completely liquid phase with a mole fraction $x^l_{2,0}$ of component 2 is instantaneously cooled from a point somewhere above the equilibrium liquidus to the point L_0 at crystallization temperature T_{cr}. Then crystallization starts and the composition of the first grown solid phase is indicated by S_0 with corresponding mole fraction $x^s_{2,0}$. As the crystallization proceeds, the liquid composition evolves toward L_{eq} due to mass conservation. Consenquently, the composition of the growing solid-phase progresses toward point S_{eq}. When the liquid arrives in point L_{eq}, the crystallization stops and the liquid is in equilibrium with the last grown solid phase at the crystal

* Corresponding author. E-mail: janlos@sci.kun.nl.

10.1021/jp025728b CCC: $22.00
Published on Web 06/21/2002

surface, which has the equilibrium composition $x^s_{2,eq}$ (S_{eq}). At that moment a metastable state has been formed with a nonhomogeneous solid phase. In fact, the previously formed solid phase has the mole fraction of component 2 varying between $x^s_{2,0}$ and $x^s_{2,eq}$, implying an average mole fraction that is lower than the equilibrium mole fraction.

The determination of the metastable state requires a kinetic approach to the crystallization process. A complete kinetic modeling of crystallization in mixed systems is a quite complex problem with many aspects, such as nucleation, kinetic segregation, diffusion in the liquid, and possible further complications, such as convection, phase separation, polymorphism, and stabilization. Actually, this complexity seems to be the main reason for the fact that usually the equilibrium approach is used, which in many cases is already complex enough. In the kinetic approach presented in this paper the complexity is handled by adopting several approximations and restrictions, to be specified later. This leads to a relatively simple kinetic model, which permits the determination of the metastable states mentioned above. The calculations according to the kinetic model provide at least a qualitative insight in the role of the kinetics in mixed crystallization processes. In addition, they give a quantitative estimate of the deviations from the equilibrium state, i.e., they provide information on how good the equilibrium prediction may be in a certain specified case.

An important aspect of the kinetic modeling is the segregation occurring at the solidification front during growth. At conditions close to equilibrium, the growth composition of the growing mixed crystal is given by the equilibrium phase diagram and one speaks of equilibrium segregration. If, however, the growth takes place at conditions far from equilibrium, which is often the case in industrial crystallization, one speaks of kinetic segregation. This nonequilibrium segregation can be represented by kinetic phase diagrams,[5] which give the growth composition of the solid phase for liquid compositions and temperatures on a kinetic liquidus below the equilibrium liquidus. Kinetic segregation has been studied by either Monte Carlo simulations based on the solid on solid model,[6] or by sets of kinetic equations[7] as well as stochastic models[8,9] for crystal growth. In refs 10 and 11, different types of kinetic phase diagrams for various model materials were presented. Most models require considerable numerical effort to find the steady-state solution, even for a binary system, whereas the results remain still subject to uncertainty since the used constants (kinetic constants and activation energies) are often not well known. Another class of models has been developed for the case of semiconductor doping, i.e., for the low concentrations limit.[12,13]

In the kinetic modeling of a crystallization process in a finite system, where the liquid composition and possibly also the temperature change continuously as the process proceeds, the actual growth composition of the solid phase has to be determined many times. Therefore it is important to have a segregation model that permits an easy determination of the growth composition for a given liquid composition and crystallization temperature. Such a model is the linear kinetic segregation (LKS) model, which has been introduced in a previous paper[14] for binary systems and will be extended here to multicomponent systems including, in addition, a condition for selecting the stable steady-state solutions. We found that the predictions of the LKS model are in good agreement with the results of Monte Carlo simulations for binary crystal growth with components A and B if the AA-bond energy in the solid state is not too much different from that of a BB-bond. For two isomorphous fat molecules which show miscibility in the solid phase this condition is fulfilled. Furthermore, despite its simplicity the LKS model is able to predict compositional kinetic phase separation, i.e., the simultaneous growth of more than one solid phase with different compositions, for eutectic or peritectic systems.

The above-described metastability is particularly inconvenient in experimental determination of equilibrium phase diagrams by calorimetric measurements such as differential scanning calorimetry (DSC). Very often it appears to be impossible to obtain agreement between theory and experiment for both the liquidus and the solidus. This has led to a strategy in which only the experimental liquidus points are used to fit the excess-energy parameters.[15]

As already mentioned, in this work we will compare the results of our kinetic model with those of the equilibrium calculation. A comparison with experimental work will be given elsewhere.[16]

The principles of the equilibrium description of the crystallization behavior in a mixed system in terms of liquid−solid equilibria can be found in many textbooks, for example refs 17, 18, and 19. The application of crystallization behavior to mixed fat systems has been described in ref 20. Since the equilibrium approach will be used as a reference for the kinetic approach, we will describe both the equilibrium and the kinetic model in a convenient formulation with one liquid phase (i.e., no phase separation in the liquid) and multiple solid phases. After the presentation of the two models in sections 2.1 and 2.2, respectively, a convenient way to characterize a metastable state is defined in section 2.3. Section 3 contains the results of calculations for several fat mixtures (blends) referring to the kinetic segregation in section 3.1, the evolution of the crystallization process represented by crystallization curves in section 3.2, and a quantitative comparison of the metastable state and the equilibrium state in section 3.3. We end with a summary and conclusions in section 4.

2. Theory

2.1. Equilibrium Model. The equilibrium model is based on the minimization of the total Gibbs free energy, G. For a multicomponent system consisting of one liquid phase, with N_c crystallizing components and possibly a solvent, and N_s different solid phases, G can be written as

$$G = G^l + G^s = G^l + \sum_{j=1}^{N_s} G^{sj} = \sum_{i=1}^{N_c} N_i^l \mu_i^l + N_{solv}^l \mu_{solv}^l + \sum_{j=1}^{N_s} \sum_{i=1}^{N_c} N_i^{sj} \mu_i^{sj} \quad (1)$$

where the superscripts l and s refer to the liquid and the solid phase, respectively, and the superscript sj refers to the jth solid phase in the system. The free energy of the solid phase, G^s, is equal to the sum of the free energies of each of the individual solid phases, G^{sj}. The different solid phases may either have different crystal structure (different polymorphs) or different compositions. Furthermore, N_i^P is the amount (in moles) of component i in phase P (l or sj) and μ_i^P is the chemical potential of that component in phase P. In the remainder the corresponding quantities for the solvent are indicated by using the subscript "solv" instead of i, e.g., N_{solv}^l and μ_{solv}^P. It is assumed that the solid phase does not contain solvent. The overall amount of component i in the system, N_i, is equal to

$$N_i = N_i^{\mathrm{l}} + \sum_{j=1}^{N_s} N_i^{sj} \tag{2}$$

for $i = 1, .., N_c$, and the total amount of all components, N, is given by

$$N = N_{\mathrm{solv}} + \sum_{i=1}^{N_c} N_i \tag{3}$$

On the other hand N is also given by

$$N = L + S = L + \sum_{j=1}^{N_s} S_j, \tag{4}$$

where L and S are the total amounts (in moles) of liquid and solid phase respectively and S_j is the amount of the jth solid phase in the system. With these definitions, the fractional amounts of the liquid phase, l, the jth solid phase, s_j, and the total solid phase, s, are given by

$$l = L/N,\ s_j = S_j/N, \text{ and } s = S/N \tag{5}$$

respectively, and the mole fractions in the liquid phase, x_i^{l} and $x_{\mathrm{solv}}^{\mathrm{l}}$, and the jth solid phase, x_i^{sj}, are equal to

$$x_i^{\mathrm{l}} = \frac{N_i^{\mathrm{l}}}{L},\ x_{\mathrm{solv}}^{\mathrm{l}} = \frac{N_{\mathrm{solv}}^{\mathrm{l}}}{L}, \text{ and } x_i^{sj} = N_i^{sj}/S_j \tag{6}$$

respectively. The overall mole fractions in the total system z_i and z_{solv} are defined by

$$z_i = \frac{N_i}{N} \text{ and } z_{\mathrm{solv}} = \frac{N_{\mathrm{solv}}}{N} \tag{7}$$

The chemical potential of component i in phase P can be written as

$$\mu_i^P = \mu_i^{P,0} + RT \ln(\gamma_i^P x_i^P) \tag{8}$$

where $\mu_i^{P,0}$ is the chemical potential of component i in the pure phase P and γ_i^P is the activity coefficient of component i in phase P. R is the gas constant and T the absolute temprature. In general, γ_i^P depends on the composition of the phase P (see below). For the minimization of G as a function of the variables N_i^{l} and N_i^{sj} one can eliminate one of the variables N_i^{sj} from eq 1 by using the constraint eq 2. This leads to the following familiar condition for the minimum of G:

$$\frac{\partial G}{\partial N_i^{\mathrm{l}}} = 0 \Rightarrow \mu_i^{\mathrm{l}} = \mu_i^{sj} \tag{9}$$

After substitution of eq 8 into eq 9 and using some thermodynamic relations we find

$$\ln\left(\frac{\gamma_i^{sj} x_i^{sj}}{\gamma_{i,\mathrm{eq}}^{\mathrm{l}} x_{i,\mathrm{eq}}^{\mathrm{l}}}\right) = \frac{\Delta H_{i,0}^{sj} \Delta T_i^{sj}}{RT_i^{sj} T} - \frac{\Delta c_{P,i} \Delta T_i^{sj}}{RT} + \frac{\Delta c_{P,i}}{R} \ln\left(\frac{T_i^{sj}}{T}\right) \tag{10}$$

where T_i^{sj} and $\Delta H_{i,0}^{sj}$ are the melting temperature and the melting enthalpy, respectively, for the pure component i and the polymorph of the jth solid phase, $\Delta c_{P,i}$ is the difference between the heat capacities of the liquid and the solid phase, and $\Delta T_i^{sj} = T_i^{sj} - T$. Usually the sum of the last two terms on the right-hand side of eq 10 is small so that these terms are often neglected. Adopting this approximation, eq 10 can be rewritten as

$$\gamma_{i,\mathrm{eq}}^{\mathrm{l}} x_{i,\mathrm{eq}}^{\mathrm{l}} = x_i^{sj} \gamma_i^{sj} \exp\left(\frac{-\Delta H_{i,0}^{sj} \Delta T_i^{sj}}{RT_i^{sj} T}\right) \quad (i = 1, .., N_c, j = 1, .., N_s) \tag{11}$$

We note that we have added the subscript "eq" to the liquid mole fractions and corresponding activity coefficients to indicate that these are the equilibrium values with respect to a solid phase of a given composition with mole fractions x_i^{sj}. This expression will also be used in the description of the nonequilibrium situation later on, since it is needed to determine the supersaturation.

Dividing eq 2 by N and using eqs 5 and 6 we find a mass balance equation that is completely defined in terms of mole fractions, namely

$$l x_{i,\mathrm{eq}}^{\mathrm{l}} + \sum_{j=1}^{N_s} s_j x_i^{sj} = z_i \quad (i = 1, .., N_c). \tag{12}$$

Finally, we have the stoichiometric relations

$$\frac{z_{\mathrm{solv}}^{\mathrm{l}}}{l} + \sum_{i=1}^{N_c} x_{i,\mathrm{eq}}^{\mathrm{l}} = 1$$

and

$$\sum_{i=1}^{N_c} x_i^{sj} = 1 \quad (j = 1,.., N_s) \tag{13}$$

where we have used that $x_{\mathrm{solv}}^{\mathrm{l}} = z_{\mathrm{solv}}/\mathrm{l}$. For given overall mole fractions z_i and z_{solv} the set of $(N_s + 1)(N_c + 1)$ equations 11, 12, and 13 forms a complete set for the $(N_s + 1)(N_c + 1)$ unknown fractions $x_{i,\mathrm{eq}}^{\mathrm{l}}$, x_i^{sj}, l, and s_j ($i = 1,.., N_c$ $j = 1,.., N_s$) to be solved.

To be able to solve the set of equations 11, 12, and 13, we still need a description of the activity coefficients γ_i^P as a function of the composition for each of the phases P. The activity coefficients are directly related to the mixing excess free energy, $G_{\mathrm{mix}}^{P,\mathrm{exc}}$. The total free energy, G^{p}, of a phase P can be written as

$$G^P = \sum_{i=1}^{N_c^P} N_i^P \mu_{i,0}^P + RT \sum_{i=1}^{N_c^P} N_i^P \ln(x_i^P) + G_{\mathrm{mix}}^{P,\mathrm{exc}} \tag{14}$$

where N_c^P is the number of components in the phase P. The second term on the right-hand side represents the ideal mixing free energy, $G_{\mathrm{mix}}^{\mathrm{id}} = -TS_{\mathrm{ideal}}^P$, where S_{ideal}^P is the ideal mixing entropy, i.e., the configurational entropy of mixing. Comparison of eq 14 with eq 1 combined with eq 8 leads to the relation

$$RT \ln(\gamma_i^P) = \frac{\partial G_{\mathrm{mix}}^{P,\mathrm{exc}}}{\partial N_i^P} \tag{15}$$

In general $G_{\mathrm{mix}}^{P,\mathrm{exc}}$ consists of an enthalpy part, $H_{\mathrm{mix}}^{P,\mathrm{exc}}$, and an entropy part, $S_{\mathrm{mix}}^{P,\mathrm{exc}}$, according to the relation

$$G_{\mathrm{mix}}^{P,\mathrm{exc}} = H_{\mathrm{mix}}^{P,\mathrm{exc}} - TS_{\mathrm{mix}}^{P,\mathrm{exc}} \tag{16}$$

If $S_{\mathrm{mix}}^{P,\mathrm{exc}}$ equals zero the solution is called regular, whereas the solution is called athermal if $H_{\mathrm{mix}}^{P,\mathrm{exc}}$ equals zero. For certain families of solid solutions, experimental and theoretical investigations have shown that $H_{\mathrm{mix}}^{P,\mathrm{exc}}$ and $S_{\mathrm{mix}}^{P,\mathrm{exc}}$ depend only weakly on the temperature and have the same sign so that there is a compensation temperature where $G_{\mathrm{mix}}^{P,\mathrm{exc}}$ is equal to zero due to enthalpy−entropy compensation.[21,22] An often used, empirical expression for the molar mixing excess free energy, $g_{\mathrm{mix}}^{P,\mathrm{exc}} = G_{\mathrm{mix}}^{P,\mathrm{exc}}/N$, is the three-suffix Margules equation.[23] For a multicomponent system, including an excess entropy term following ref 21, this model can be extended to

$$g_{\mathrm{mix}}^{P,\mathrm{exc}} = \sum_{i=1}^{N_c}\sum_{i'=i+1}^{N_c}\left(1-\frac{T}{\theta_{ii'}}\right)\times R\tilde{T}_{ii'}\left(\phi_{ii'}^{P,\mathrm{exc}}\frac{x_{i'}^{P}}{x_i^P+x_{i'}^P}+\phi_{i'i}^{P,\mathrm{exc}}\frac{x_i^P}{x_i^P+x_{i'}^P}\right)x_i^P\,x_{i'}^P \quad (17)$$

where $\theta_{ii'}$ is the compensation temperature for the binary mixture of the components i and i', $\tilde{T}_{ii'}^{P} = (T_i^P + T_{i'}^P)/2$ is the average melting temperature of this pair for phase P and $\phi_{ii'}^{P,\mathrm{exc}}$ and $\phi_{i'i}^{P,\mathrm{exc}}$ are dimensionless excess energy parameters. The parameter $\phi_{ii'}^{P,\mathrm{exc}}$ is equal to $\Phi_{ii'}^{P,\mathrm{exc}}/R\tilde{T}_{ii'}^{P}$ where $\Phi_{ii'}^{P,\mathrm{exc}}$ is proportional to the excess bond energy per ii' bond in a dilute solution of component i into the phase P of component i'. Likewise, $\phi_{i'i}^{P,\mathrm{exc}}$ refers to a dilute solution of component i' into i. By substitution of eq 17 into eq 15 we find

$$\gamma_i^P = \exp\left(-\frac{g_{\mathrm{mix}}^{P,\mathrm{exc}}}{RT}+\sum_{i'=1,i'\neq i}^{N_c^P}\left(1-\frac{T}{\theta_{ii'}}\right)\frac{\tilde{T}_{ii'}}{T}\times\left(\frac{\phi_{i'i}^{P,\mathrm{exc}}((x_i^P)^2+2x_i^P\,x_{i'}^P)+\phi_{ii'}^{P,\mathrm{exc}}(x_{i'}^P)^2}{(x_i^P+x_{i'}^P)^2}\right)x_{i'}^P\right) \quad (18)$$

In literature, the calculation of the equilibrium state in a multicomponent system from the above equations is also known as flash calculation. For complex systems, i.e., systems with many components and more than one polymorph and/or compositional phase separation, the flash calculation can be quite complicated since in general it is not a priori known how many solid phases are present in the state of minimal free energy. This problem has been tackled in ref 24.

2.2. Kinetic Model. As already mentioned, it is unlikely that the equilibrium state is actually realized in a multicomponent liquid−solid system due to the very low diffusion rate in the solid phase. To overcome the complexity of a kinetic modeling we adopt two main assumptions: (i) the temperature is homogeneous and (ii) the composition of the liquid phase is homogeneous. These assumptions apply when heat transport and mass diffusion in the liquid are much faster than the kinetics at solidification front and imply an important simplification of a kinetic description. For fats these assumptions are reasonable,[25,26] in particular for stirred conditions. Our kinetic description consists of the linear kinetic segregation (LKS) model and mass conservation equations, as described below. For simplicity we consider crystallization at constant temperature. However, also adiabatic conditions, i.e., no heat exchange with the surroundings, can be readily incorporated within the framework of the present model.

During crystal growth, the growth units, i.e., atoms or molecules, at the interface make transformations from the liquid to the solid state and vice versa, denoted as attachment and detachment or adsorption and desorption, respectively. The basic assumption that leads to the LKS model[14] is to consider these processes as transformations between bulk phases, neglecting the fact that the intermediate states at the interface are not bulk states. Then, according to the principle of microscopic reversibility, the ratio of the attachment flux, J_i^+, and the detachment flux, J_i^-, for a component i is given by

$$\frac{J_i^+}{J_i^-} = \exp\left(\frac{\Delta\mu_i}{RT}\right) \quad (19)$$

where $\Delta\mu_i = \mu_i^{\mathrm{l}} - \mu_i^{\mathrm{s}}$ is the chemical potential difference between the liquid and the solid state for component i. Using eq 8 leads to the well-known expression

$$\Delta\mu_i = RT\ln\left(\frac{\gamma_i^{\mathrm{l}}x_i^{\mathrm{l}}}{\gamma_{i,\mathrm{eq}}^{\mathrm{l}}x_{i,\mathrm{eq}}^{\mathrm{l}}}\right) \quad (20)$$

where the product $\gamma_{i,\mathrm{eq}}^{\mathrm{l}}x_{i,\mathrm{eq}}^{\mathrm{l}}$ is given by eq 11. According to the chemical reaction rate theory the attachment flux can be written as

$$J_i^+ = K_i^+ x_i^{\mathrm{l}} = K_{i,0}^+\gamma_i^{\mathrm{l}}x_i^{\mathrm{l}} \quad (21)$$

where $K_i^+ = K_{i,0}^+\gamma_i^{\mathrm{l}}$ is an attachment probability per unit surface area with dimensions $\mathrm{m}^{-2}\,\mathrm{s}^{-1}$ and $K_{i,0}^+$ is supposed to be equal to the attachment probability for the case of growth from a pure melt of component i. In many papers on kinetic segregation, the attachment probability K_i^+ is assumed to be equal for each component, which seems reasonable for isomorphous components. This assumption is in agreement with eq 21 if $K_{i,0}^+$ is assumed to be equal for each component and the mixing in the liquid is ideal, implying $\gamma_i^{\mathrm{l}} = 1$. After substitution of eqs 20 and 21 into eq 19 we find that the detachment flux J_i^- is equal to $K_{i,0}^+\gamma_{i,\mathrm{eq}}^{\mathrm{l}}x_{i,\mathrm{eq}}^{\mathrm{l}}$, so that the net flux or growth rate R_i for component i becomes

$$R_i = J_i^+ - J_i^- = K_{i,0}^+(\gamma_i^{\mathrm{l}}x_i^{\mathrm{l}} - \gamma_{i,\mathrm{eq}}^{\mathrm{l,gr}}x_{i,\mathrm{eq}}^{\mathrm{l,gr}}) = K_{i,0}^+\sigma_i \quad (22)$$

where $\sigma_i = \gamma_i^{\mathrm{l}}x_i^{\mathrm{l}} - \gamma_{i,\mathrm{eq}}^{\mathrm{l,gr}}x_{i,\mathrm{eq}}^{\mathrm{l,gr}}$ is the absolute supersaturation for component i. The total growth rate R is then given by

$$R = \sum_{i=1}^{N_c}R_i = \sum_{i=1}^{N_c}K_{i,0}^+(\gamma_i^{\mathrm{l}}x_i^{\mathrm{l}} - \gamma_{i,\mathrm{eq}}^{\mathrm{l,gr}}x_{i,\mathrm{eq}}^{\mathrm{l,gr}}) \quad (23)$$

The ratio of the mole fractions of component 1 and any other component i in the growing solid phase is determined by the ratio of growth rates for these components, i.e., $x_1^{\mathrm{s,gr}}/x_i^{\mathrm{s,gr}} = R_1/R_i$ or

$$\frac{x_1^{\mathrm{s,gr}}}{x_i^{\mathrm{s,gr}}} = \kappa_{1i}\frac{\gamma_1^{\mathrm{l}}x_1^{\mathrm{l}} - \gamma_{1,\mathrm{eq}}^{\mathrm{l,gr}}x_{1,\mathrm{eq}}^{\mathrm{l,gr}}}{\gamma_i^{\mathrm{l}}x_i^{\mathrm{l}} - \gamma_{i,\mathrm{eq}}^{\mathrm{l,gr}}x_{i,\mathrm{eq}}^{\mathrm{l,gr}}} \quad (i = 2, .., N_c) \quad (24)$$

where we have defined the kinetic constant ratio $\kappa_{1i,0} \equiv K_{1,0}^+/K_{i,0}^+$. In eqs (22−24) we have added the superscript gr to indicate that it concerns the composition of the solid phase that is actually growing and not the bulk solid phase. Hence, $x_i^{\mathrm{s,gr}}$ is the mole fraction of component i in the growing solid phase and $x_{i,\mathrm{eq}}^{\mathrm{l,gr}}$ and $\gamma_{i,\mathrm{eq}}^{\mathrm{l,gr}}$ are the equilibrium mole fraction and corresponding activity coefficient of component i in the liquid with respect to the growing solid phase. Together with the

stoichiometric condition for the solid phase, i.e., $\sum_{i=1}^{N_c} x_i^{s,gr} = 1$, and eqs 11 and 18 to express $\gamma_{i,eq}^{l,gr} x_{i,eq}^{l,gr}$ in terms of $x_i^{s,gr}$, the set of equations 24 can be solved numerically for the N_c mole fractions $x_i^{s,gr}$ for given kinetic constants ratios κ_{1i}.

As will be shown in the next section, for large excess energies eq 24 can have more than one solution, implying compositional kinetic phase separation, i.e., the simultaneous growth of more than one solid phase with different compositions. However, not every solution of eq 24 is physically acceptable. First, for a physically relevant solution all growth rate R_i should be positive. Next, the solution should correspond to a stable steady-state solution. The criterion for this is derived as follows.

The increase of the amount of component i that has crystallized, N_i^s, is given by

$$\frac{dN_i^s}{dt} = R_i(\boldsymbol{x}^{s,gr}) \quad (i = 1, .., N_c) \tag{25}$$

where we have adopted the vector notation $\boldsymbol{x}^{s,gr} = (x_1^{s,gr}, x_2^{s,gr}, ...)$. For the steady-state regime it holds that $x_i^{s,gr} = N_i^s/N^s$ with $N^s = \sum_i N_i^s$. Combined with eq 25, this leads to the following set of coupled first order differential equations for $x_i^{s,gr}$:

$$\frac{dx_i^{s,gr}}{dt} = \frac{1}{N^s}(R_i - x_i^{s,gr}R) \equiv \frac{1}{N^s}F_i(\boldsymbol{x}^{s,gr}) \quad (i = 1,.., N_c) \tag{26}$$

where we have defined the functions $F_i(\boldsymbol{x}^{s,gr}) \equiv (R_i - x_i^{s,gr}R)$, which for a steady-state solution (fulfilling the constraint $\sum x_i^{s,gr} = 1$) have to be equal to zero. Note that these solutions are equivalent to those of eq 24. Then, using the standard theory of first order differential equations, the steady-state solution is stable if the real parts of all the eigenvalues of the Jacobian of the vector function $\boldsymbol{F}(\boldsymbol{x}^{s,gr})$ at the solution, restricted to the invariant subspace defined by $\sum x_i^{s,gr} = 1$, are negative. The solutions of eq 24, which do not fulfill this criterion, will not grow as a bulk phase.

For example, for a binary system it is easily verified that for the given form of the excess energy (eq 17), the equation $F_1(x_1^{s,gr}, x_2^{s,gr}) = F_1(x_2^{s,gr}) = 0$ has either one or three solutions for $x_2^{s,gr} = 1 - x_1^{s,gr} \in [0, 1]$ (except for some special points). Note that $F_1(0) = -K_{2,0}^+ \gamma_2^l x_2^l < 0$ and $F_1(1) = K_{1,0}^+ \gamma_1^l x_1^l > 0$. If F_1 has only one root, this root corresponds to a stable steady state solution according to the above criterion and only one phase is growing (if also $R_1, R_2 > 0$). If F_1 has three roots $x_2^{s1,gr} < x_2^{s2,gr} < x_2^{s3,gr}$, then the middle one corresponds to an unstable steady-state solution whereas both others correspond to stable steady-state solutions yielding the simultaneous growth of two phases, each of them enriched in one of the two components.

Apart from this compositional kinetic phase separation one may also have kinetic phase separation due to the simultaneous growth of different polymorphs. To find all the possible growing solid phases, eq 24 should be solved for each of the possible polymorphs.

To complete the kinetic description we have to add a set of mass conservation equations. We assume that the formation of solid phase starts at $t = 0$ from a completely liquid initial state. During crystallization, the solid fraction s increases at the cost of the liquid fraction $l = 1 - s$. In our approach the independent variable is not the time t but the solid fraction s, i.e., the evolution of the relevant quantities involved is described as a function of s. We use this approach since we are primarily interested in the amounts and compositions of the various phases in the final state and less in how much time (within a reasonable time scale) it takes to reach this state. Moreover, a description of the nucleation process and the corresponding induction time can be avoided in this way. Assume that at a given moment, N_s solid phases are growing simultaneously, with compositions $x_i^{sj,gr}$ ($j = 1, .., N_s$) being the physically acceptable solutions of eq 24, and let ds_j be a small amount of the jth solid phase that is formed in a certain small time interval. Conservation of mass implies

$$\sum_{j=1}^{N_s} x_i^{sj,gr} ds_j + d(lx_i^l) = \bar{x}_i^{sj,gr} ds + x_i^l dl + l dx_i^l = 0 \tag{27}$$

for $i = 1, .., N_c$ where $ds = \sum_j ds_j$ is the total fraction of solid phase that is formed in the given time interval and $\bar{x}_i^{s,gr}$ is defined as the average mole fraction of component i in this total fraction:

$$\bar{x}_i^{s,gr} = \sum_j^{N_s} \frac{ds_j}{ds} x_i^{sj,gr} \tag{28}$$

Using $dl = -ds$, eq 27 yields

$$\frac{dx_i^l}{ds} = \frac{x_i^l - \bar{x}_i^{s,gr}}{1 - s} \tag{29}$$

If kinetic phase separation occurs we have to know the weight factors ds_j/ds in order to determine $\bar{x}_i^s$. This is a complicated problem since these weight factors do not only depend on the instantaneous growth rates but also on the evolution of the growth surfaces for each of the growing phases. Therefore, to keep the present work concise we will treat the cases where kinetic phase separation occurs in a separate paper,[29] where we will derive a model for the determination of the weight factors ds_j/ds as a function of s. In the present paper we will limit ourselves to cases where no kinetic phase separation occurs, implying $N_s = 1$ and $ds = ds_1$ and $\bar{x}_i^{s,gr} = x_i^{s1,gr} \equiv x_i^{s,gr}$. One single solid phase will evolve if only one crystal modification occurs and compositional phase separation is avoided by assuming low excess energies or taking a crystallization temperature that is above the eutectic (or peritectic) temperature.

For fats, there are three main classes of crystal modifications (polymorphs), namely the α-, the β'-, and the β-modification.[30,31] However, in general during the primary crystallization, i.e., before post growth recrystallization, one of the modifications will have the largest nucleation and/or growth rate and will therefore dominate the crystallization process. If this modification is not the most stable one, a transition to a more stable modification may take place after the primary crystallization (Ostwald rule of stages). This indeed occurs for many fat mixtures at high undercooling where after the rapid formation of the relatively unstable α-phase a slower transition to the more stable β'- or β-phase takes place. Here we will not consider such transitions but focus on the modeling of the primary crystallization process with only one modification.

Summarizing, the kinetic model describing the mixed crystallization process for cases without kinetic phase separation consists of the sets of equations 24 and 29 with $\bar{x}_i^{s,gr} = x_i^{s1,gr} \equiv x_i^{s,gr}$, eqs 11 and 18 to express $\gamma_{i,eq}^{l,gr} x_{i,eq}^{l,gr}$ in terms of the $x_i^{s,gr}$, and the stoichiometric condition for the mole fractions of the growing solid phase. Solving these equations numerically yields crystallization curves, describing the evolution of R^s, x_i^l, and $x_i^{s,gr}$ as a function of the solid fraction s.

TABLE 1: Melting Temperature T_{melt} (in °C) and Melting Enthalpy ΔH_{melt} (in kJ/mole) for the β-Modification of PPP, MyPP, SOS, and POP

	PPP	MyPP	SOS	POP
T^{β}_{melt}	64.50	57.96	44.90	37.70
ΔH^{β}_{melt}	169.04	148.22	134.87	120.55

2.3. Characterization of the Metastable State. For the general case with N_s solid phases, important characterizations of the metastable state are given by the number of solid phases that have been formed, the corresponding solid fractions s_j, and the total solid-phase fraction $s = \sum_j^{N_s} s_j$, as well as the final liquid composition, i.e., the mole fractions in the remaining liquid after the metastable state has been reached, which we denote as $x^{l}_{i,ms}$. The characterization can be completed by the average mole fractions in the solid phase(s), $\bar{x}_i^{sj}$ ($i = 1, ..N_c$), given by

$$\bar{x}_i^{sj} = \frac{1}{s_j}\int_0^{s_j} x_i^{s,gr}(s_j')\,ds_j' \tag{30}$$

and the corresponding nonhomogeneities, Δx_i^{sj} ($i = 1,..N_c$), which we define as

$$\Delta x_i^{sj} = \sqrt{\frac{1}{s_j}\int_0^{s_j} (x_i^{sj,gr}(s_j') - \bar{x}_i^{sj})^2\,ds_j'} \tag{31}$$

similar to the definition of the standard deviation. This characterization allows for a straightforward comparison with the equilibrium state.

3. Results

We take fat mixtures as model systems. The initial liquid composition is equal to the overall composition, i.e., $x_i^{l}(0) \equiv x^{l}_{i,0} = z_i$. Following ref 20, the mixing behavior in the liquid is assumed to be ideal, i.e., $G^{l,exc} = 0$, and the solid solutions are assumed to be regular, i.e., the entropy terms proportional to T in eq 17 are neglected. This assumption is supported by the fact that usually the variation of the total excess energy within the temperature range of interest is small.[21] Furthermore, all kinetic constants $K^{+}_{i,0}$ are taken equal to one (assuming an appropriate time unit), implying $\kappa_{1i} = 1$ for $i = 2, .., N_c$, unless mentioned explicitly.

We have done calculations for fat mixtures with up to four components from the group PPP, MyPP, SOS, and POP assuming the β-modification with a nomenclature specified in Appendix A. Their thermodynamic data are listed in Table 1. The excess energy parameters were chosen arbitrarily, within a range of typical values, to illustrate their influence. Furthermore, we have done calculations for three other blends assuming the β'-modification, namely two ternary blends and one palm oil blend with 10 components, which we denote as blend 1, blend 2 and blend 3, respectively. The composition of these blends and the thermodynamic data for the β'-modification with realistic excess energy parameters, taken from ref 20, are given in Appendix A.

In several cases the crystallization temperature T_{cr} is given indirectly by what we call the reference undercooling ΔT_0, which is defined as

$$\Delta T_0 = T_{eq,max} - T_{cr} \tag{32}$$

where $T_{eq,max}$ is the equilibrium temperature for the system consisting of a fraction $1 - z_{solv}$ of the component with the highest melting temperature which is dissolved in a solvent with fraction z_{solv}. Hence, for a system without solvent $T_{eq,max}$ is equal to the melting temperature of that component. The definition of ΔT_0 is illustrated in Figure 1.

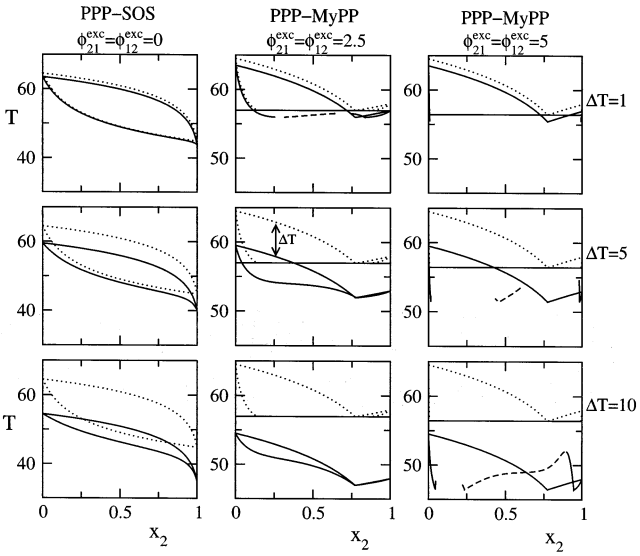

Figure 2. Kinetic phase diagrams (full lines) for the binary fat systems PPP−SOS (1−2) and PPP−MyPP (1−2) for ideal and nonideal mixing behavior, respectively, with excess energy parameters $\phi_{ii'}^{exc}$ as indicated above the top graph for each column of graphs. The undercooling ΔT for the graphs in a row is indicated in the right-hand side margin. In all cases the kinetic constant ratio κ_{12} is set equal to one. The dotted lines give the equilibrium phase diagram. The dashed lines represent unstable solutions of eq 24.

3.1. Kinetic Phase Diagrams. With the LKS model (eq 24) one can construct kinetic phase diagrams. These diagrams give the composition of the solid phase that is growing for liquid compositions along a given liquidus line, denoted as the kinetic liquidus, which is below the equilibrium liquidus. The resulting solidus line is denoted as the kinetic solidus.

Figure 2 shows the equilibrium and kinetic phase diagrams for the binary systems PPP−SOS and PPP−MyPP for undercoolings equal to $\Delta T = 1$, 5, and 10 K. For the PPP−SOS system, the mixing behavior in the solid phase was taken to be ideal, i.e., $\phi_{21}^{s,exc} = \phi_{12}^{s,exc} = 0$, whereas for the PPP−MyPP system, the excess energy parameters were taken equal to $\phi_{21}^{s,exc} = \phi_{12}^{s,exc} = 2.5$ and $\phi_{21}^{s,exc} = \phi_{12}^{s,exc} = 5$. In each graph the kinetic liquidus (upper full line) is the result of a downward shifted equilibrium liquidus (upper dotted line) over a distance ΔT. The other full lines are the corresponding kinetic solidi. For small undercooling, $\Delta T = 1$ *K*, the kinetic phase diagram is nearly equal to the equilibrium phase diagram. Actually, it is an intrinsic property of the LKS model that for $\Delta T \to 0$ the kinetic phase diagram coincides with the equilibrium phase diagram, independent of the kinetic constant ratio κ_{12},[14] as it should be. In fact, in the limit of zero driving force no kinetic deviation from the equilibrium composition is to be expected. For increasing ΔT the kinetic solidus rapidly approaches the kinetic liquidus. This tendency was also found in Monte Carlo simulations for binary systems of semiconductors,[32] but is more pronounced for fats due to the relatively high $\Delta H_i/RT$ ratio for fats. According to eq 11, the larger this ratio, the more rapidly the equilibrium concentration tends to zero for increasing undercooling and, owing to eq 24, the more rapidly the solid-phase composition becomes equal to the liquid composition.

For the PPP−MyPP system the equilibrium phase diagram is eutectic for the two settings of the excess energy parameters (see Figure 2). In both cases there is a wide ranging miscibility

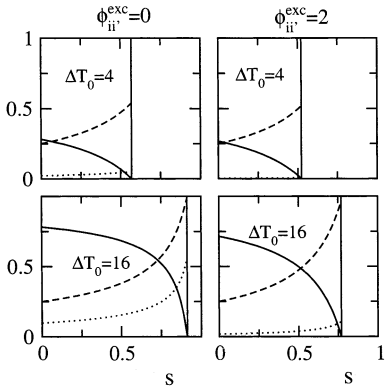

Figure 3. Crystallization curves showing the evolution of the crystallization process for the binary system PPP−SOS (1−2) with initial mole fractions ($x_{1,0}^{l}$, $x_{2,0}^{l}$) = (0.75, 0.25) for different reference undercoolings ΔT_0 (in K) as indicated in the graphs and different settings of the excess energy parameters, indicated above the top graphs for each column. The various lines give the evolution of the growth rate (full line) and the mole fractions of component 2 (SOS) in the liquid (dashed line) and in the growing solid phase (dotted line) as a function of the solid fraction *s*. The vertical line indicates the end of the crystallization process where the growth rate becomes equal to zero.

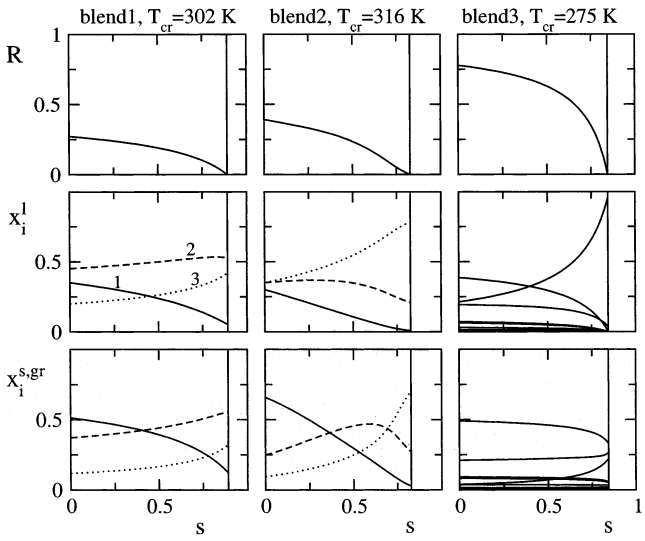

Figure 4. Crystallization curves showing the evolution of the crystallization process of the three blends specified in Appendix A. The crystallization curves give the growth rate *R* (top graphs), the mole fractions in the liquid, x_i^l, (middle graphs), and the growing solid phase, $x_i^{s,gr}$, (bottom graphs) as a function of the solid fraction *s*. The full, dashed, and dotted lines, used for blend 1 and blend 2, are for the components 1, 2, and 3, respectively, in order of decreasing pure component melting temperature. The crystallization temperature (in K) for each of the three blends is indicated above the top graphs.

gap. The larger the excess parameters, the larger this miscibility gap between the PPP-rich and the MyPP-rich solid phases. For $\phi_{BA}^{exc} = \phi_{AB}^{exc} = 2.5$, we see that for $\Delta T = 1$ K the range of the miscibility gap is reduced with respect to the equilibrium situation and that for $\Delta T = 5$ and 10 K all solid-phase compositions can be obtained kinetically. As for the ideal mixing case, the growth composition tends toward the liquid composition for increasing undercooling. Qualitatively, the same is observed for $\phi_{BA}^{exc} = \phi_{AB}^{exc} = 5$, but here the phase separation tendency is stronger and a much larger undercooling is needed to eliminate the miscibility gap. Furthermore, especially the second and the third graph in the third column clearly show that for liquid compositions lying on a certain part of the kinetic liquidus there are three growth compositions possible, i.e., eq 24 has three solutions in these cases. There are two solutions that correspond to a PPP-rich and a MyPP-rich growth composition and a third solution with a growth composition between, indicated by the dashed line in these graphs. The PPP-rich and MyPP-rich solutions correspond to stable steady-state solutions, according to the criterion given in section 2, and imply compositional kinetic phase separation. This may either give domain formation or separate crystallites. The third solution corresponds to an unstable steady-state solution.

3.2. Crystallization Curves. Examples of crystallization curves are shown in Figure 3. These curves were calculated for the binary system PPP−SOS with initial mole fractions ($x_{PPP,0}^{l}$, $x_{SOS,0}^{l}$) = (0.75, 0.25) for ideal and nonideal mixing behavior in the solid phase and several crystallization temperatures. The vertical line indicates where the growth rate *R* (full line) becomes equal to zero and gives the solid fraction of the final, metastable state. The dashed and dotted lines give the mole fractions of SOS in the liquid and the growing solid phase, respectively. We can see that the compositions of the liquid and the growing solid phase approach each other for increasing undercooling and that this tendency decreases for increasing excess energy. These results regarding the miscibility are in agreement with those in Figure 2. The final solid fraction for nonideal mixing is lower than that for ideal mixing. For increasing excess energy the solid phase tends to become pure PPP. In this limit the final solid fraction tends to $s = x_{PPP,0}^{l} =$ 0.75 for increasing undercooling as long as the crystallization temperature lies above the eutectic temperature, implying complete crystallization of only the PPP component.

Figure 4 shows the crystallization curves for the three blends from Appendix A for crystallization temperatures yielding a high final solid fraction. As we can see, for the ternary blends the solid phase is strongly nonhomogeneous, in particular for blend 2. For blend 3 the solid phase is more homogeneous, implying that in this case the metastable state is closer to the equilibrium state. The results for blend 2 give a nice and typical illustration of what can happen. At first the growing solid phase is rich in the component with the highest melting temperature, SPS. When the concentration of that component in the liquid has decreased far enough, the component with second highest melting temperature, SSLa, starts to become dominant in the growing solid phase. Finally, the liquid has become so rich of the third component, PLaLa, that the last grown solid phase is rich in this component.

3.3. Metastable State versus Equilibrium State. The solid fraction of the equilibrium state, s_{eq}, for the case with only one solid phase is given by the well-known "lever-rule":

$$s_{eq} = \frac{x_{i,eq}^{l} - z_i^{l}}{x_{i,eq}^{l} - x_{i,eq}^{s}} \tag{33}$$

which directly follows from the mass balance of eq 12. The subscript "eq" is added to refer to the equilibrium state. Equation 33 holds if the point of the overall composition (e.g., L_0 in Figure 1) lies between the solidus and the liquidus. Above the liquidus $s_{eq} = 0$ and below the solidus $s_{eq} = 1$. The solid fraction of the metastable state with only one solid phase, s_{ms}, follows by integration of eq 29. We find

$$s_{ms} = 1 - \exp\left(\int_{x_{i,0}^{l}}^{x_{i,ms}^{l}} \frac{dx_i^{l}}{x_i^{l} - x_i^{s,gr}(\mathbf{x}^{l})}\right) \tag{34}$$

where $x^{l}_{i,ms}$ is the concentration in the final liquid and where we have used the vector notation $\mathbf{x^l} = (x^{l}_{1}, x^{l}_{2}, ..)$. According to the Gibbs phase rule, for a binary system ($i = 1, 2$) at a given temperature the equilibrium concentrations $x^{l}_{i,eq}$ and $x^{s}_{i,eq}$ are uniquely determined. However, for systems with more than two components the liquid- and solid-phase compositions yielding equality of the chemical potentials of the liquid and the solid-phase lie on a $N_c - 2$ dimensional manifold. In the equilibrium model the equilibrium concentrations for a given overall composition are fixed by the additional mass balance equations. However, in the kinetic model the final concentrations in the liquid, $x^{l}_{i,ms}$, which are in equilibrium with the last grown solid phase at the surface, depend on the crystallization path and will in general not be equal to $x^{l}_{i,eq}$ for systems with more than two components.

A simple approximate expression for s_{ms} can be obtained from eq 34 by replacing $x_i^{s,gr}(\mathbf{x^l})$ by a constant, "average" value equal to $\tilde{x}_i^{s,gr} = (x^{s,gr}_{i,0} + x^{s,gr}_{i,ms})/2$, where $x^{s,gr}_{i,ms}$ is the concentration of component i in the last grown solid phase. Then the integration in eq 34 can be carried out analytically and we find the following approximation $\tilde{s}_{ms}$ for s_{ms}:

$$\tilde{s}_{ms} = \frac{x^{l}_{i,ms} - x^{l}_{i,0}}{x^{l}_{i,ms} - \tilde{x}_i^{s,gr}} \tag{35}$$

For a binary system we have $x^{l}_{i,ms} = x^{l}_{i,eq}$ as was pointed out above. Since $x^{l}_{i,0} = z_i$, the only difference between eq 33 and eq 35 is that $x^{s}_{i,eq}$ is replaced by $\tilde{x}_i^{s,gr}$. Considering again the situation in Figure 1, it is clear that $\tilde{x}_2^{s,gr} = (x^{s,gr}_{2,0} + x^{s}_{2,eq})/2 < x^{s}_{2,eq}$, which implies that $\tilde{s}_{ms}$ is smaller than s_{eq}. This result appears to be characteristic. Numerically, we found that only extreme (unrealistic) values of the kinetic constants ratio can lead to a state with $s_{ms} > s_{eq}$. Hence, although the approximation (eq 35) may be quantitatively not very accurate, it demonstrates in a transparent way that in general the solid fraction predicted by the kinetic model is lower than the equilibrium solid fraction. A much more accurate, but less transparent expression for s_{ms} can be obtained by using a linear interpolation for $x_i^{s,gr}$ as a function of x^{l}_{i}.

In Figure 5 the solid fractions of the metastable state as a function of the initial composition, calculated by numerically solving the kinetic model equations, are shown for the binary system PPP−SOS with and without solvent for several ΔT_0 and $\phi^{exc}_{ii'}$ and for three values of the kinetic constants ratio κ_{12}. To compare the equilibrium solid fraction is also given. In all cases $s_{ms} < s_{eq}$ and the effect of taking κ_{12} a factor 10 (!) larger or smaller is relatively small. This agrees with the relatively small effect that the kinetic constants ratio has on the kinetic phase diagrams for not too large undercooling (ref 14). The difference between s_{ms} and s_{eq} is maximal for ideal mixing without solvent. The effect of the excess energy can be understood by realizing that for complete demixing the solid phase would be pure. In that case the solid fraction is completely fixed by the solubility of the crystallizing component and s_{ms} would be equal to s_{eq}. In the presence of a solvent the solid fraction has a maximum equal to $1 - z_{solv}$. According to eq 29 the rate of change of the liquid concentrations is proportional to $1/(1 - s)$. Hence, the rate of change of the liquid concentrations and consequently the nonhomogeneity of the solid phase are relatively small for low solid fractions with respect to the case where s is closer to 1. This implies that the metastable state is closer to the equilibrium state. The difference between s_{ms} and s_{eq} is thus relatively small for low solid fractions.

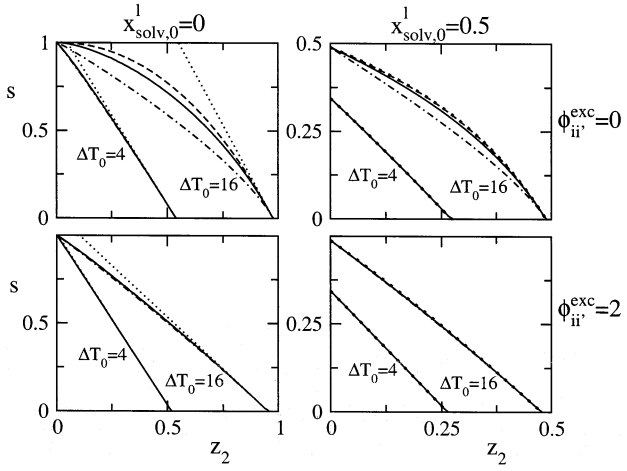

Figure 5. Solid fraction s_{ms} for the binary system PPP−SOS (1−2) as a function of the overall mole fraction $z_2 = z_{SOS}$ for two different reference undercoolings, two settings of the excess energy parameters (indicated in right-hand side margin for the upper and lower graphs), and different choices for the kinetic constant ratio κ_{12}, without solvent (left graphs) and with solvent (right graphs). The full lines give the results for $\kappa_{12} = 1$ whereas the dashed and chain dashed lines give the results for $\kappa_{12} = 10$ and $\kappa_{12} = 0.1$, respectively. The dotted lines give the equilibrium solid fractions.

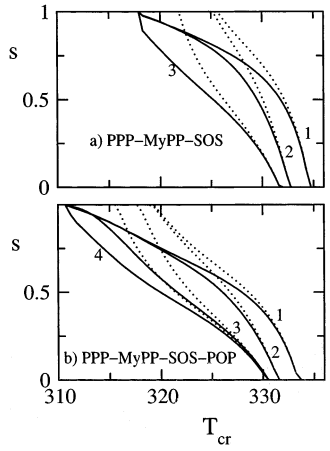

Figure 6. Solid fraction s_{ms} (full lines) as a function of the reference undercooling ΔT_0 for the ternary system PPP−MyPP−SOS (a) with initial compositions $x^{l}_{0} = (0.5, 0.25, 0.25)$ (line 1), (0.25, 0.5, 0.25) (line 2), and (0.25, 0.25, 0.5) (line 3) and for the quaternary system PPP−MyPP−SOS−POP (b) with initial compositions $x^{l}_{0} = (0.4, 0.2, 0.2, 0.2)$ (line 1), (0.2, 0.4, 0.2, 0.2) (line 2), (0.2, 0.2, 0.4, 0.2) (line 3), and (0.2, 0.2, 0.2, 0.4) (line 4). All excess energy parameters were set equal to zero. The dotted lines give the respective equilibrium solid fraction.

We have also calculated the solid fraction as a function of the crystallization temperature. The results of these calculations for the ternary system PPP−MyPP−SOS and the quaternary system PPP−MyPP−SOS−POP, assuming ideal miscibility, are shown in Figure 6 for various initial compositions. Again, $s_{ms} < s_{eq}$ and the difference between s_{ms} and s_{eq} is largest for a large solid fraction and can be as much as ≃0.4. The differences in s_{eq} for the different compositions can be explained by the difference in the average melting temperature defined as $T_{av} = \sum_i z_i T_i$. The larger T_{av}, the larger is s_{eq}, as to be expected. The same holds for s_{ms}.

A complete characterization of the metastable state as a function of the crystallization temperature for the three blends from Appendix A is given in Figure 7. Again the results are

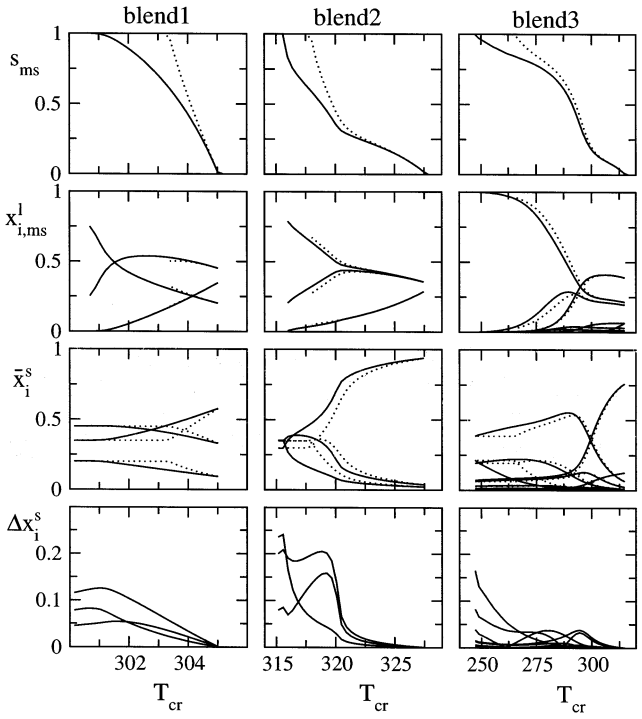

Figure 7. Metastable state (full lines) compared with the equilibrium state (dotted lines) as a function of the crystallization temperature for the three blends from Appendix A. For convenience, the labels refer only to the metastable state. The graphs in the top row give the solid fraction. The final liquid concentrations and the average composition of the solid phase are given in the graphs in the second and the third row, respectively. The nonhomogeneity is given in the graphs in the bottom row.

compared with the corresponding equilibrium predictions, except for the nonhomogeneity which is, of course, zero for the equilibrium state. For blend 3 the deviation from the equilibrium state is somewhat smaller than for the ternary blends. This is in agreement with the results in Figure 4, which shows a relatively homogeneous solid phase for blend 3. This can be explained by the relatively large amount of the low melting point component LLL in blend 3, which acts more or less as a solvent at temperatures well above its melting point. As we pointed out in the discussion of Figure 5, the presence of a solvent leads to a more homogeneneous solid phase. For all three blends, the liquid concentrations $x^l_{i,ms}$ are rather close to the equilibrium liquid concentrations, at least within the temperature interval where the equilibrium solid fraction is less than one, i.e., where the liquid is present. Within the temperature range where $s_{eq} = 1$ and $s_{ms} < 1$, the kinetic model predicts final liquid compositions which can deviate considerably from any of the equilibrium compositions at higher temperatures, in particular for blend 1. The deviation of the average composition of the solid phase with respect to the equilibrium composition is larger than that for the liquid composition. Again, the deviation is largest for high solid fractions, the relative difference, $|\bar{x}^s_i - x^s_{i,eq}|/x^s_{i,eq}$, can amount to more than 0.5 for blend 2. The nonhomogeneity is rather large for all three blends and increases for increasing solid fraction. One can show that if x^s_i would depend linearly on s and the difference between the maximum value of x^s_i and its minimum value would be equal to δx^s_i, then Δx^s_i would be equal to $\delta x^s_i/\sqrt{3}$ according to eq 31. Hence, the variation in the composition is of the order $\sqrt{3}\Delta x^s_i$, which leads to the conclusion that the nonhomogeneity is indeed significant for all three blends, most of all for blend 2, which is in agreement with the result in Figure 4.

4. Summary and Conclusions

A simple kinetic model has been defined for describing the crystallization behavior in a multicomponent system, including a model for nonequilibrium segregation. The model can be used to determine the evolution of a crystallization process in a finite, multicomponent system from given pure-component melting temperatures and enthalpies, and excess energy parameters. This evolution is represented by crystallization curves, which give the growth rate, the liquid composition, and composition of the growing solid phase as a function of the increasing solid fraction. The resulting final state is a metastable state with (in general) a nonhomogeneous solid phase for which a convenient characterization has been defined, permitting a straightforward comparison with the equilibrium state.

We have assumed a homogeneous temperature and liquid composition, so that the model particularly applies to systems with slow surface kinetics at stirred conditions. However, the model is flexible enough to include the effect of volume diffusion.[16] Furthermore, we have assumed isothermal conditions, but the model can easily be adapted for adiabatic conditions.

A previously defined kinetic segregation model for binary systems, the LKS model, has been extended to multicomponent systems, including an extra condition for selecting the stable solutions. According to the LKS model, immiscibility increases for increasing undercooling. However, for sufficiently large mixing excess energy and not too large undercooling, it predicts compositional kinetic phase separation, i.e., the simultaneous growth of more than one solid phase with different compositions. But for further increased undercooling this phase separation is overruled by the kinetics and vanishes.

The crystallization curves, as calculated by the kinetic model, show that a significant nonhomogeneity can occur in the solid phase, especially for components that mix well, i.e., with small excess energy parameters. This induces a reduced final solid fraction with respect to the equilibrium prediction. The difference in the prediction of the solid fraction according to the kinetic and the equilibrium model increases for increasing solid fraction and is, to a large extent, independent of the choice of the kinetic constant ratios. The difference in the solid fractions is maximal for components that mix well and can amount to e 0.4 for the cases considered here. The presence of a solvent favors the homogeniety of the solid phase, reducing the difference between the metastable state and the equilibrium state. Further differences between the metastable state and the equilibrium state, as regards the final liquid composition and the average composition of the solid phase, are also correlated with the nonhomogeneity and can be significant.

Acknowledgment. This work has been sponsored by Unilever Research Vlaardingen, The Netherlands. We thank Prof. T. Janssen, Dr. A. Fasolino, Dr. F. Gandolfo, and J. G. Blok for discussions and assistence.

Appendix

In this work, the names of the fat components (triglycerides) are taken according to a convention of nomenclature. A triglyceride is denoted by a three-letter code representing the three fatty acids that are esterified with the glycerol. La, My, P, S, and O stand for lauric, myristic, palmitic, stearic, and oleic acid with chain lengths of 12, 14, 16, 18, and 18 carbon atoms, respectively.

The tables below give the data for the three fat blends used for the calculations in section 3. The pure-component melting

TABLE 2: Blend 1 and Blend 2

	Blend 1			Blend 2		
	SOS	POS	POP	SSLa	SPS	PLaLa
z_i	0.35	0.45	0.2	0.30	0.35	0.35
T_i	309.15	302.35	300.15	335.65	324.75	316.15
ΔH_i	97.90	94.30	98.50	132.60	102.00	71.30
ϕ_{1i}^{exc}	0.0	0.0	0.26	0.0	2.1	2.0
ϕ_{2i}^{exc}	0.0	0.0	0.0	2.1	0.0	1.5
ϕ_{3i}^{exc}	0.26	0.0	0.0	2.0	1.5	0.0

TABLE 3: Blend 3

	LLL	LaOP	OOS	PLaP	POA	POO	POP	PPO	PPP	PPS
z_i	0.213	0.014	0.030	0.006	0.010	0.193	0.386	0.064	0.072	0.012
T_i	248.1	294.6	290.8	324.6	311.1	284.0	299.6	307.1	330.4	331.7
ΔH_i	42.65	59.94	77.45	104.60	105.50	64.82	89.78	100.80	133.40	124.80
ϕ_{1i}^{exc}	0.00	2.10	0.00	3.10	0.20	0.00	0.26	0.26	1.14	0.26
ϕ_{2i}^{exc}	2.10	0.00	2.10	3.60	2.10	1.24	0.40	2.25	1.36	2.25
ϕ_{3i}^{exc}	0.00	2.10	0.00	3.13	0.20	0.00	0.26	0.26	1.14	0.26
ϕ_{4i}^{exc}	3.10	3.60	3.13	0.00	3.13	2.25	1.36	1.36	0.47	1.36
ϕ_{5i}^{exc}	0.20	2.10	0.20	3.13	0.00	0.00	0.26	0.26	1.14	0.26
ϕ_{6i}^{exc}	0.00	1.24	0.00	2.25	0.00	0.00	0.00	0.00	0.33	0.00
ϕ_{7i}^{exc}	0.26	0.40	0.26	1.36	0.26	0.00	0.00	0.33	0.00	0.33
ϕ_{8i}^{exc}	0.26	2.25	0.26	1.36	0.26	0.00	0.33	0.00	0.00	0.00
ϕ_{9i}^{exc}	1.14	1.36	1.14	0.47	1.14	0.33	0.00	0.00	0.00	0.00
ϕ_{10i}^{exc}	0.26	2.25	0.26	1.36	0.26	0.00	0.33	0.00	0.00	0.00

temperatures, T_i (in K), melting heats, ΔH_i (in kJ/mol), and the dimensionless excess energy parameters, $\phi_{ii'}$, are for the β'-modification, all taken from ref 20. The first row gives the overall mole fractions, z_i.

Note Added after Print Publication. Equations 5, 6, and 31 were given incorrectly in the original work (published on the Web 6/21/2002; Vol. 106, No. 29, pp 7321−7330) and are now shown correctly. An Addition and Correction appears in the December 5, 2002 issue (Vol. 106, No. 48).

References and Notes

(1) Kitaigorodskii, A. I. *Mixed Crystals*; Springer-Verlag: Berlin, 1984.
(2) van Eikeren, P. In *Chiral separations: applications and technology*; Ahuja, S., Ed.; American Chemical Society: Washington, DC, 1997; Chapter 2.
(3) Gilbert, E. P.; Reynolds, P. A.; Brown, A. S.; White, J. W. *Chem. Phys. Lett.* **1996**, *255*, 373.
(4) Dorset, D. L.; Snyder, R. G. *J. Phys. Chem. B* **1999**, *103*, 3282.
(5) *Kinetic Phase Diagrams*; Chvoj, Z.; Šesták, J.; Tříska, A., Eds.; Elsevier: Amsterdam, 1991.
(6) Cherepanova, T. A. *J. Cryst. Growth* **1980**, *59*, 371.
(7) Pfeiffer, H.; Haubenreisser, W. *Phys. Status Solidi B* **1980**, *101*, 253.
(8) Chvoj, Z. *Cryst. Res. Technol.* **1986**, *21*, 1003.
(9) Chvoj, Z. *Cryst. Res. Technol.* **1987**, *22*, 709.
(10) Cherepanova, T. A.; Didrikhsons, G. T. *Krist. Tech.* **1979**, *14*, 1501.
(11) Cherepanova, T. A.; Didrikhsons, G. T. *Phys. Status Solidi A* **1980**, *59*, 633.
(12) Reitano, R.; Smith, P. M.; Aziz, M. J. *J. Appl. Phys.* **1994**, *76*, 3, 1518.
(13) Jackson, K. A.; Gilmer, G. H.; Temkin, D. E.; Beatty, K. M. *J. Cryst. Growth* **1996**, *163*, 461.
(14) Los, J. H.; Flöter, E. *Phys. Chem. Chem. Phys.* **1999**, *1*, 4251.
(15) Bouwstra, J. A.; van Genderen, A. C. G.; Brouwer, N.; Oonk, H. A. J. *Thermochim. Acta* **1980**, *38*, 97.
(16) Los, J. H. et al., work in progress.
(17) Guggenheim, E. A. *Thermodynamics*, 5th ed.; North-Holland: Amsterdam, 1967.
(18) Wallace, D. C. *Thermodynamics of Crystals*; Wiley: New York, 1972.
(19) Rosenberger, F. *Fundamentals of Crystal Growth I*; Springer: Berlin, 1979.
(20) Wesdorp, L. H. Liquid-multiple solid-phase equilibria in fats. Ph.D. Thesis, University Delft, The Netherlands, 1990.
(21) Oonk, H. A. J.; Mondieig, D.; Haget, Y.; Cueveas-Diarte, M. A. *J. Chem. Phys.* **1998**, *108*(2), 715.
(22) van der Kemp, W. J. M.; Blok, J. G.; van der Linde, P. R.; Oonk, H. A. J.; Schuijff, A.; Verdonk, M. L. *Thermochim. Acta* **1993**, *225*, 17.
(23) Prausnitz, J. M. *Molecular Thermodynamics of Fluid Phase Equilibria*; Prentice Hall: Englewood Cliffs, NJ, 1986.
(24) Michelsen, M. L. *Fluid Phase Equilibria* **1982**, *9*, 1. Michelsen, M. L. *Fluid Phase Equilibria* **1982**, *9*, 21.
(25) Knoester, M.; de Bruyne, P.; v. d. Tempel, M. *J. Cryst. Growth* **1968**, *3*, 776.
(26) van Putte, K. P. A. M.; Bakker, B. H. *Jaocs* **1987**, *64*, 1138.
(27) Wilson, H. A. *Philos. Mag.* **1900**, *50*, 238.
(28) Frenkel, J. *Phys. Z. Sowjetunion* **1932**, *1*, 498.
(29) Los, J. H.; van Enckevort, W. J. P.; Vlieg, E.; Flöter, E.; Gandolfo, F. G. *J. Phys. Chem. B* **2002**, *106*, 7331.
(30) Chapman, D. *Chem. Rev.* **1962**, *62*, 433.
(31) Larsson, K. *Arkiv. Kemi* **1964**, *23*, 35.
(32) Cherepanova, T. A.; Dzelme, J. B. *Cryst. Res. Technol.* **1981**, *16*, 399.